1521-0103/384/3/445–454$35.00
THE JOURNAL OF PHARMACOLOGY AND EXPERIMENTAL THERAPEUTICS

dx.doi.org/10.1124/jpet.122.001298
J Pharmacol Exp Ther 384:445–454, March 2023

Neutralizing MIP3α Reduces Renal Immune Cell Infiltration and Progressive Renal Injury in Young Obese Dahl Salt-Sensitive Rats

Ubong S. Ekperikpe, Bibek Poudel, Corbin A. Shields, Sautan Mandal, Denise C. Cornelius, and Jan M. Williams

Departments of Pharmacology and Toxicology and Emergency Medicine, University of Mississippi Medical Center, Jackson, Mississippi

Received August 8, 2022; accepted November 23, 2022

ABSTRACT

Recently, we reported that the early progression of renal injury in obese Dahl salt-sensitive leptin receptor mutant (SS^{LepR}mutant) rats was associated with increased macrophage inflammatory protein 3-α (MIP3α) expression prior to puberty. Therefore, this study tested the hypothesis that MIP3α plays a role in recruiting immune cells, thereby triggering renal inflammation and early progressive renal injury in SS^{LepR}mutant rats prior to puberty. Four-week-old Dahl salt-sensitive (SS) and SS^{LepR}mutant rats either served as control (IgG; intraperitoneal, every other day) or received MIP3α-neutralizing antibody (MNA; 100 μg/kg) for 4 weeks. MNA reduced circulating and renal MIP3α levels and proinflammatory immune cells by 50%. Although MNA treatment did not affect blood glucose and plasma cholesterol levels, MNA markedly decreased insulin resistance and triglyceride levels in SS^{LepR}mutant rats. We observed no differences in mean arterial pressure (MAP) between SS and SS^{LepR}mutant rats, and MNA had no effect on MAP in either strain. Proteinuria was significantly increased in SS^{LepR}mutant rats versus SS rats over the course of the study. Treatment with MNA markedly decreased proteinuria in SS^{LepR}mutant rats while not affecting SS rats. Also, MNA decreased glomerular and tubular injury and renal fibrosis in SS^{LepR}mutant rats while not affecting SS rats. Overall, these data indicate that MIP3α plays an important role in renal inflammation during the early progression of renal injury in obese SS^{LepR}mutant rats prior to puberty. These data also suggest that MIP3α may be a novel therapeutic target to inhibit insulin resistance and prevent progressive proteinuria in obese children.

SIGNIFICANCE STATEMENT

Childhood obesity is increasing at an alarming rate and is now being associated with renal disease. Although most studies have focused on the mechanisms of renal injury associated with adult obesity, few studies have examined the mechanisms of renal injury involved during childhood obesity. In the current study, we observed that the progression of renal injury in obese Dahl salt-sensitive leptin receptor mutant rats was associated with an increase in MIP3α, a chemokine, before puberty, and inhibition of MIP3α markedly reduced renal injury.

Introduction

In recent decades, obesity has become an epidemic globally and in the United States (Ogden et al., 2015; Ogden et al., 2016). The prevalence of obesity has risen not only in adults but also in children (Cattaneo et al., 2010). According to the World Health Organization, more obese and overweight children have died than underweight children due to breathing difficulties, elevated risk of fractures, hypertension, and early markers of cardiovascular disease and insulin resistance. Obese patients have an increased risk to develop diabetes and hypertension, the two leading causes of kidney disease (Kramer et al., 2006; Srivastava, 2006). Childhood obesity is positively correlated with markers of renal injury such as elevated serum creatinine and microalbuminuria (Ferris et al., 2007; Savino et al., 2010; Kaneko et al., 2011; Önerli Salman et al., 2019). Interestingly, renal injury in obese children and adolescents starts long before the development of hypertension or diabetes. Therefore, it is necessary to identify novel targets to prevent early progressive renal disease in this unique population. Recently, we reported that the Dahl salt-sensitive leptin receptor mutant (SS^{LepR}mutant) rat develops renal injury without hyperglycemia and elevations in arterial pressure, prior to puberty, and is therefore a novel model to study mechanisms of childhood obesity-induced renal disease (McPherson et al., 2016; McPherson et al., 2019; McPherson et al., 2020; Poudel et al., 2020; Poudel et al., 2022).

This work was financially supported by National Institutes of Health National Institute of Diabetes and Digestive and Kidney Diseases [Grant R01-DK109133] (to J.M.W.) and the National Heart, Lung, and Blood Institute [Grant R01-HL151407] (to D.C.C.). The work performed through the UMMC Molecular and Genomics Facility is supported, in part, by funds from National Institutes of Health National Institute of General Medical Sciences, including Mississippi INBRE [Grant P20-GM103476], Obesity, Cardiorenal and Metabolic Diseases-COBRE [Grant P20-GM104357], and Mississippi Center of Excellence in Perinatal Research (MS-CEPR)-COBRE [Grant P20-GM121334].

No author has an actual or perceived conflict of interest with the contents of this article

dx.doi.org/10.1124/jpet.122.001298.

ABBREVIATIONS: Cr_{Cl}, creatinine clearance; DC, dendritic cell; IL, interleukin; KIM-1, kidney injury molecule-1; MAP, mean arterial pressure; MIP3α, macrophage inflammatory protein 3-α; MNA, MIP3α-neutralizing antibody; NGAL, neutrophil gelatinase-associated lipocalin; SS, Dahl salt-sensitive; SS^{LepR}mutant, Dahl salt-sensitive leptin receptor mutant.

An early hallmark characteristic of obesity-induced renal disease is elevations in glomerular filtration rate (renal hyperfiltration) (Hostetter et al., 1982; Kasiske and Napier, 1985). We hypothesized that renal hyperfiltration damages various renal cells such as podocytes and tubular cells, which are a source of proinflammatory cytokines (Rayego-Mateos et al., 2020). In support of our hypothesis, studies from our laboratory have demonstrated that early progressive proteinuria in obese SS^{LepR}mutant rats was associated with renal hyperfiltration and inflammatory cytokines such as macrophage inflammatory protein 3-α (MIP3α) (McPherson et al., 2020; Brown et al., 2021). Moreover, prevention of renal hyperfiltration in SS^{LepR}mutant rats prior to puberty slowed the progression of glomerular injury and decreased renal MIP3α levels (Brown et al., 2021). MIP3α is a low-molecular-weight chemotactic cytokine that recruits dendritic cells (DCs) and lymphocytes (Th17s, regulatory T cells, and B cells) (Wiede et al., 2013) and is secreted by podocytes and tubular cells, as well as immune cells such as macrophages (Nandi et al., 2014). However, the role of MIP3α in the progression of obesity-induced renal injury has not been studied. Therefore, the goal of the current study was to test the hypothesis that MIP3α plays a role in recruiting immune cells, thereby triggering renal inflammation and early progressive renal injury in SS^{LepR}mutant rats prior to puberty.

Methods

General. Experiments were performed on a total of 59 female and male Dahl salt-sensitive (SS) and SS^{LepR}mutant rats. Both rat strains were generated from our in-house colony of heterozygous SS^{LepR}mutant rats, which were originally created at the Medical College of Wisconsin with the zinc finger nuclease technology (McPherson et al., 2016). Genotyping was done by the Molecular and Genomics Facility of the University at Mississippi Medical Center. The rats were given free access to food and water for the entire study. Rats were fed a 1% NaCl diet (Envigo, Madison, WI). MIP3α-neutralizing antibody (MNA) and IgG isotype control were purchased from R&D Systems (Minneapolis, MN). The rats were housed in the Laboratory Animal Facility of the University of Mississippi Medical Center, which is approved by the American Association for the Accreditation of Laboratory Animal Care. All protocols were approved by the University of Mississippi Medical Center Institutional Animal Care and Use Committee.

Protocol. These experiments were carried out on 4-week-old female and male SS and SS^{LepR}mutant rats. At baseline, rats were weighed and placed in metabolic cages overnight to collect urine for the determination of proteinuria using the Bradford method (Bio-Rad Laboratories, Hercules, CA). Blood was collected from the tail vein to measure nonfasting blood glucose levels (glucometer from Bayer HealthCare; Mishwaka, IN). After the collection of baseline data, SS and SS^{LepR}mutant rats were randomly separated into four groups as follows: 1) SS and 2) SS^{LepR}mutant rats serving as control (IgG; 100 μg/kg i.p., every other day) and 3) SS and 4) SS^{LepR}mutant rats receiving MNA 100 μg/kg i.p., every other day, for 4 weeks. The doses of MNA and IgG were selected from a previous study (Hu et al., 2016). Every 2 weeks, nonfasting blood glucose and proteinuria were measured in the rats. Urine collected at the end of the protocol were used to measure the excretion rates of kidney injury molecule 1 (KIM-1; Abcam, Waltham, MA), neutrophil gelatinase-associated lipocalin (NGAL; Abcam), albumin (Abcam), and nephrin (NPB2-76751, Novus Biologicals, Littleton, CO) via ELISA according to the manufacturer's recommendations. Glomerular filtration rate was assessed via creatinine clearance (Cr_{Cl}) (Bioassay Systems, Hayward, CA).

At the end of the study, rats were anesthetized, and a catheter was inserted into the carotid artery to measure mean arterial pressure (MAP). After a 24-hour recovery period, catheters were connected to pressure transducers (MLT0699, ADInstruments, Colorado Springs, CO) coupled to a computerized PowerLab data-acquisition system (ADInstruments). After a 30-minute equilibration period, MAP was recorded continuously for 30 minutes. Then, a final blood sample was drawn from the abdominal aorta for the measurement of plasma cholesterol (Cayman Chemical, Ann Arbor, MI), triglyceride (Cayman Chemical), insulin (Mercodia rat insulin ELISA, Uppsala, Sweden), and MIP3α (Bio-Rad Laboratories, Hercules, CA) concentrations. Next, the kidneys were perfused with saline until they appeared visibly pale. The kidneys were collected and weighed. The right kidney was cut into two equal halves; one half was fixed in 10% neutral buffered formalin solution for histologic analysis. The other half was snap-frozen in liquid nitrogen and stored at −80°C. Renal cytokines were measured using the Bio-Plex Pro Rat Cytokine 5-Plex Assay Reagent Kit on a Bio-Rad Bio-Plex 200 system as described by the manufacturer's protocol (Bio-Rad Laboratories). The cytokines measured were MIP3α, interleukin (IL)-2, IL-4, IL-10, and IL-17. The left kidney was used to measure the renal infiltration of immune cells as described below.

Renal Immune Cell Isolation and Flow Cytometry. Immune cells from the left kidneys of control and MNA-treated SS and SS^{LepR}mutant rats were isolated as previously described (Poudel et al., 2020). Briefly, the kidneys were minced in RPMI-1640 containing 0.1% collagenase and 10 μg/ml DNAse 1. These were homogenized, filtered through a 100-μm strainer, incubated at 37°C for 30 minutes, and subsequently filtered through 70-μm and 40-μm strainers. Mononuclear cells were separated by Percoll density gradient centrifugation at 1200 rpm for 30 minutes at 25°C. The pellet obtained was washed and resuspended in 1 mL fluorescence-activated cell sorter buffer, after which immune cells were counted using an Automated Cell Counter and Image Cytometer (Nexcelom Bioscience, Lawrence, MA.). Mononuclear cells were stained with viability (Viobility 405/520 for macrophage and dendritic cells, 1:50; 405/452 for lymphocytes, 1:50) fixable dyes (Miltenyi Biotec, Auburn, CA) for 20 minutes at 4°C to identify live cells. The macrophage panel consisted of the following antibodies: anti-rat CD68-PE-Vio770 (1:10; Miltenyi Biotec), anti-rat CD86-PE (1:50; Miltenyi Biotec), and mouse anti-rat CD163-FITC (1:50; Bio-Rad Laboratories). The DC panel consisted of the following antibodies: anti-rat CD103-APC (1:10; Miltenyi Biotec), anti-rat CD86-PE (1:50; Miltenyi Biotec), and mouse anti-rat CD80-BV421 (1:10; BD Biosciences, Haryana, India). The lymphocyte panel consisted of the following antibodies: anti-rat CD3-VioGreen (1:10; Miltenyi Biotec) for total T cells, anti-rat CD4-FITC (1:10; Miltenyi Biotec) for total T helper cells, anti-rat CD8a-APC-Vio770 (1:50; Miltenyi Biotec) for cytotoxic T cells, mouse anti-rat CD25 PE (1:50; BD Biosciences), mouse anti-rat RORγT PerCP (1:2; R and D systems, Minneapolis, MN) for Th17 cells, mouse anti-rat FOXP3-AlexaFluor-647 (1:2; R and D systems, Minneapolis, MN) for regulatory T cells, and anti-rat CD45R-PE-Vio770 (1:10; Miltenyi Biotec) for total B cells. Flow

cytometry was carried out using the Miltenyi MACSQuant Analyzer 10 (Miltenyi Biotec), and data were analyzed using FlowLogic software (Miltenyi Biotec).

Renal Histology. Paraffin-embedded kidney sections were prepared from half of the right kidneys collected from SS and SS^{LepR}mutant rats. Kidney sections were cut into 5-μm sections and stained with periodic acid-Schiff and Picrosirius red. Thirty glomeruli per periodic acid-Schiff section were scored blindly, on a scale of 0–4 to assess glomerular injury, where 0 represented a normal glomerulus, 1 represented a 25% loss, 2 represented a 50% loss, 3 represented a 75% loss, and 4 represented a greater than 75% loss of capillaries in the glomerular tuft (McPherson et al., 2016; Spires et al., 2018). To assess the extent of renal cortical and medullary fibrosis from Picrosirius red–stained sections, 10 representative images per kidney section per animal were taken with a SeBa microscope equipped with a colored camera (Laxco Inc., North Creek, WA). We analyzed for the percentage of each image stained red (collagen) by identifying the animal whose kidney had the most collagen. This was used to set a threshold for red staining in the sections using NIS-Elements D 3.0 software (McPherson et al., 2016; Spires et al., 2018). Next, those same thresholding parameters were used for the red staining on each kidney image per rat in the study to measure renal fibrosis.

Statistical Analysis. The data are presented as mean values ± S.D. Statistical analysis was performed using GraphPad Prism 8 (GraphPad Software, San Diego, CA). The significance of the difference in mean values for a single timepoint was determined by two-way ANOVA followed by Holm-Sidak's multiple-comparisons test. Time-course changes in protein excretion were compared from baseline, between and within strains, using three-way ANOVA followed by Tukey's multiple-comparisons test. P values of <0.05 were considered significantly different.

Results

Flow Cytometry. The flow cytometry gating strategy for immune cell infiltration is provided in Fig. 1. After gating for the mononuclear cell population using forward scatter and side scatter, dead cells were excluded using viability staining and doublet exclusion. From this population, $CD3^+$ cells were gated as T lymphocytes, and $CD4^+$ T Helper cells and $CD8^+$ cytotoxic T cells were identified from the $CD3^+$ cell population. From the $CD4^+$ T Helper cell population, $CD25^+FOXP3^+$ cells were identified as regulatory T cells, whereas $CD25^-ROR\gamma T^+$ cells were identified as Th17s. $CD45R^+$ B cells were identified from the $CD3^-$ cell population. Also, from the $CD3^-$ population, $CD68^+$ and $CD103^+$ cells were identified as macrophages and DCs, respectively. $CD68^+CD86^+$ and $CD68^+CD163^+$ cells were identified as M1 and M2 macrophages, respectively. $CD103^+CD80^+$ and $CD103^+CD86^+$ cells were identified as stimulatory DCs.

Measurement of Circulating and Renal MIP3α. The effects of chronic MNA administration on plasma and renal MIP3α are shown in Fig. 2. Plasma and renal MIP3α were markedly greater in control SS^{LepR}mutant rats versus SS rats, and chronic MNA administration only decreased MIP3α in the plasma and kidneys of SS^{LepR}mutant rats (Fig. 2, A and B).

Metabolic Endpoints. The effects of chronic MNA administration on metabolic endpoints are presented in Table 1. There was a marked increase in body weight in control SS^{LepR} mutant rats in comparison with their SS counterparts, and MNA treatment did not affect body weight in either strain. We detected no differences in blood glucose levels in any of the groups. We observed an almost 10-fold increase in plasma insulin in control SS^{LepR}mutant rats in comparison with SS rats, and the administration of MNA markedly reduced plasma insulin levels in SS^{LepR}mutant rats by over 50% while not affecting SS rats. Plasma triglycerides were over 6 times higher in control SS^{LepR}mutant rats compared with SS counterparts (467 ± 91 mg/dL versus 70 ± 28 mg/dL, respectively), and the administration of MNA decreased plasma triglycerides by over 50% (210 ± 30 mg/dL) while not affecting SS rats (71 ± 24 mg/dL). There was a marked increase in plasma total cholesterol in control SS^{LepR}mutant rats in comparison with SS rats (252 ± 46 versus 143 ± 38 mg/dL, respectively), and the administration of MNA did not affect plasma total cholesterol in either strain.

Measurement of Mean Arterial Pressure and Markers of Renal Injury. The effects of MNA administration on MAP and markers of renal injury (proteinuria and albuminuria) are presented in Fig. 3. There were no marked differences in MAP among control and MNA-treated SS and SS^{LepR}mutant rats (Fig. 3A). At baseline, we detected no differences in protein excretion between SS and SS^{LepR}mutant rats. During the course of the study, proteinuria rose from 41 ± 7 mg/d to 426 ± 47 mg/d in control SS^{LepR}mutant rats compared with control SS rats, where proteinuria only rose from 10 ± 3 mg/d to 51 ± 16 mg/d. Chronic MNA administration decreased proteinuria by over 50% in SS^{LepR}mutant rats while not affecting SS rats (Fig. 3B). At the end of the study, we observed an over 30-fold increase in albumin excretion in control SS^{LepR}mutant rats in comparison with SS rats, and chronic administration of MNA resulted in a near fivefold decrease in albumin excretion in SS^{LepR}mutant rats while not affecting SS rats (Fig. 3C).

Renal Function Assessment and Markers of Glomerular and Tubular Injury. The effects of MNA on creatinine clearance (Cr_{Cl}), as well as markers of glomerular and tubular injury, are presented in Fig. 4. There was a marked increase in Cr_{Cl} in control SS^{LepR}mutant rats in comparison with SS rats. Chronic MNA administration did not affect Cr_{Cl} in SS^{LepR}mutant rats and SS rats (Fig. 4A). We detected a fourfold increase in nephrin excretion in control SS^{LepR}mutant rats in comparison with SS rats, and the administration of MNA decreased nephrin excretion by about 50% in SS^{LepR}mutant rats while not affecting SS rats (Fig. 4B). There was a marked increase in excretion of urinary markers of tubular injury (KIM-1 and NGAL) in control SS^{LepR}mutant rats in comparison with their SS counterparts (Fig. 4, C and D). The chronic administration of MNA markedly decreased KIM-1 and NGAL excretion in SS^{LepR}mutant rats while not affecting the SS counterparts.

Renal Histology. Representative images and a corresponding analysis of renal histopathology in control and MNA-treated SS and SS^{LepR}mutant rats are shown in Fig. 5. The kidneys from control SS^{LepR}mutant rats showed increased mesangial expansion and glomerular injury in comparison with their SS counterparts (Fig. 5, A and D), and chronic MNA administration significantly reduced glomerular injury in SS^{LepR} mutant rats. Greater fibrosis was seen in the renal cortex (Fig. 5, B and E) and renal medulla (Fig. 5, C and F) of SS^{LepR} mutant rats in comparison with their SS counterparts, and

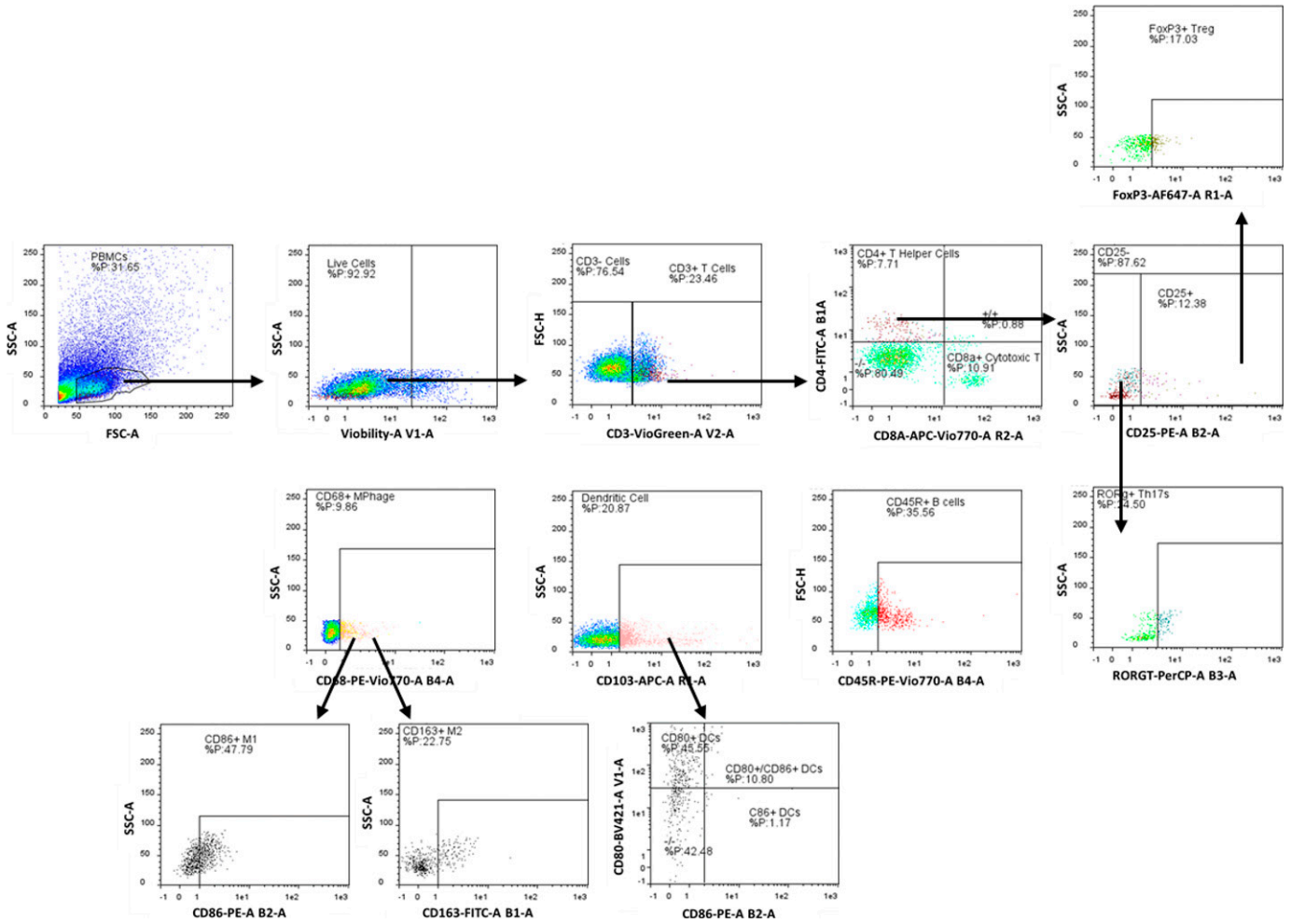

Fig. 1. Flow cytometry gating strategy: Flow cytometry was carried out for macrophage, dendritic cell (DC), and lymphocyte panels. After gating for mononuclear cells using forward scatter (FSC) and side scatter (SSC), dead cells were excluded using viability staining, and doublets were excluded. $CD45^+$ staining was used to gate for total lymphocytes. From this population, gates were placed for $CD3^-$ cells and $CD3^+$ T cells. $CD45R^+$ B cells were identified in the $CD3^-$ cell population, and $CD4^+$ T helper and $CD8^+$ cytotoxic T subsets were identified within the $CD3^+$ T-cell population. From the $CD4^+$ T helper cell population, $CD25^+/FOXP3^+$ cells were identified as regulatory T cells (Tregs), whereas $CD25^-/ROR\gamma T^+$ cells were identified as IL-17–producing T helper cells (Th17s). Additionally, singlet $CD45^+/CD3^-$ cells were gated. Within this population, $CD68^+$ and $CD103^+$ were identified as macrophages and DCs, respectively. $CD68^+/CD86^+$ and $CD68^+/CD163^+$ cells were identified as M1 and M2 macrophages, respectively. $CD103^+/CD80^+$ and $CD103^+/CD86^+$ cells were identified as stimulatory DCs.

chronic MNA administration reduced cortical and medullary interstitial fibrosis.

Measurement of Renal Immune Cell Infiltration. The effects of MNA on renal immune cell infiltration are shown in Figs. 6 and 7. There was a marked increase in renal $CD103^+$ and $CD103^+/CD80^+$ DCs in control SS^{LepR}mutant rats in comparison with SS rats, with no noteworthy differences detected in $CD103^+/CD86^+$ DCs. Chronic administration of MNA markedly reduced the renal infiltration of these DCs without affecting SS rats (Fig. 6, A and B). Renal total macrophages were significantly increased in control SS^{LepR} mutant rats versus SS rats. Similar results were observed with M1 and M2 macrophages (Fig. 6, E and F). The administration of MNA significantly decreased the infiltration of total and M1 macrophages, but not M2, in SS^{LepR}mutant rats (Fig. 6, D and E).

The effect of the administration of MNA on the renal infiltration of various lymphocytes is presented in Fig. 7. We detected a marked increase in the renal infiltration of total T cells, Th17s, and cytotoxic T cells in control SS^{LepR}mutant rats in comparison with SS rats. The chronic administration of MNA markedly reduced the renal infiltration of Th17s and cytotoxic T cells, but not total T cells, in SS^{LepR}mutant rats (Fig. 7, A, B, and E). No differences were detected in total T Helper cells or regulatory T cells across the groups (Fig. 7, D and F). Total B cells were markedly increased in the kidneys of control SS^{LepR}mutant rats in comparison with SS rats. The administration of MNA only reduced the renal infiltration of B cells in SS^{LepR}mutant rats (Fig. 7C).

Renal Cytokine Measurements. The effects of chronic MNA administration on other renal cytokines are presented in Fig. 8. There was a marked decrease in renal IL-10 in control SS^{LepR}mutant rats in comparison with SS rats. Chronic MNA treatment did not affect renal IL-10 in SS^{LepR}mutant rats (Fig. 8A). Similar to IL-10, we noticed a 50% reduction in renal IL-4 in control SS^{LepR}mutant rats versus SS rats, and chronic MNA treatment did not affect renal IL-4 in SS^{LepR}mutant rats (Fig. 8B). There were no differences in renal IL-2 or IL-17 expression for both control and MNA-treated SS and SS^{LepR}mutant rats (Fig. 8, C and D).

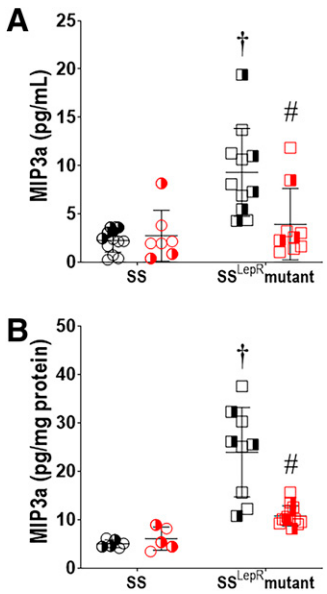

Fig. 2. Effects of chronic treatment with an MNA on plasma and renal expression of MIP3α levels in SS and obese SS^{LepR}mutant rats. Control SS and SS^{LepR}mutant rats are represented by circles and squares outlined in black, respectively, and MNA-treated rats are represented by circles and squares outlined in red. Female and male rats in each group are represented by partially filled and open symbols, respectively. (A) plasma MIP3α levels and (B) renal MIPa levels. Values are means ± S.D. The significance of the difference in mean values for a single timepoint was determined by a two-way ANOVA followed by Holm-Sidak's multiple comparisons test. $P < 0.05$ was considered significantly different. †, a significant difference from the corresponding value in SS rats within the same treatment; #, a significant difference from the corresponding value in control-treated rats within the same strain.

Discussion

Obese adults and children are susceptible to renal disease independent of diabetes or hypertension (Kramer et al., 2006; Srivastava, 2006; Kovesdy et al., 2017). Although studies have focused on mechanisms of renal disease in adult obesity, little effort has been put into studying renal disease associated with childhood/prepubertal obesity. A major characteristic of obese patients is renal hyperfiltration (Ferris et al., 2007; Eirin et al., 2017; van Bommel et al., 2020). Studies have demonstrated that obesity-induced hyperfiltration leads to injury of specialized cells of the glomerulus, such as the podocytes, and tubular epithelial cells, which are a source of proinflammatory mediators (Brown et al., 2021). Recently, we reported that early progressive renal injury was associated with renal hyperfiltration, glomerular injury, renal macrophage infiltration, and increased renal MIP3α expression in obese SS^{LepR}mutant rats before puberty (McPherson et al., 2016; Poudel et al., 2020; Brown et al., 2021; Poudel et al., 2022). Moreover, preventing renal hyperfiltration reduced MIP3α and renal disease during the prepubescent stage (Brown et al., 2021). Thus, the aim of the current study was to determine the role of MIP3α during the early progression of renal injury in SS^{LepR}mutant rats prior to puberty. The administration of MNA decreased circulating and renal levels of MIP3α by over 50% in SS^{LepR} mutant rats. Additionally, MNA administration reduced the renal infiltration of various immune cells (i.e., DCs, macrophages, Th17s, cytotoxic T cells, and B cells) in SS^{LepR}mutant rats and significantly decreased renal injury in SS^{LepR}mutant rats. In addition, the administration of MNA improved metabolic parameters in SS^{LepR}mutant rats by decreasing insulin resistance and plasma triglyceride levels. Taken together, these results show that the neutralizing MIP3α ameliorates metabolic endpoints and decreases renal inflammation and renal injury in SS^{LepR}mutant rats before puberty.

Insulin is essential for the maintenance of physiologic levels of triglycerides as it promotes triglyceride storage while preventing its breakdown in adipose tissues (Czech et al., 2013). The SS^{LepR}mutant rats displayed features of metabolic syndrome, and MNA administration decreased hyperinsulinemia/insulin resistance and dyslipidemia while not affecting their body weight or blood glucose levels. A plausible explanation for this is that the anti-inflammatory effects of MNA improved insulin resistance in SS^{LepR}mutant rats. Hyperinsulinemia is a known indicator of systemic insulin resistance (Czech, 2017; Petersen and Shulman, 2018). The chemokine system contributes to insulin resistance during obesity by regulating immune cell recruitment, thereby triggering inflammation and impairing insulin sensitivity (Cancello et al., 2005; Huber et al., 2008; Neels et al., 2009; Kitade et al., 2012; Ota, 2013). This is supported by studies that show that inhibiting the chemokine signaling pathway, MCP1-CCR2, improved insulin sensitivity, whereas the overexpression of MCP1-CCR2 stimulated insulin resistance in mice (Kamei et al., 2006; Kanda et al., 2006; Weisberg et al., 2006). Although information on the role of MIP3α in metabolic syndrome is limited, a study reported that MIP3α is elevated in the serum of obese mice (Burke et al., 2015). In the current study, plasma MIP3α was elevated in SS^{LepR}mutant rats, and the administration of MNA decreased plasma MIP3α and reduced hyperinsulinemia, suggesting a relationship between plasma MIP3α and obesity-related

TABLE 1
Effects of chronic MNA on metabolic parameters in SS rats and obese SS^{LepR}mutant rats.
Values are means ± S.D.

	Control Treatment		MNA Treatment	
Metabolic Parameters	SS	SS^{LepR}mutant	SS	SS^{LepR}mutant
Total animals	12	10	12	15
(Female, male)	(7, 5)	(4, 6)	(7, 5)	(7, 8)
Body Weight (g)	202 ± 13	310 ± 14^{a}	220 ± 13	304 ± 9^{a}
Glucose (mg/dl)	98 ± 3	97 ± 4	101 ± 6	96 ± 3
Insulin (ng/ml)	1.0 ± 0.3	11.0 ± 2.0^{a}	1.0 ± 0.2	4.0 ± 0.6^{a,b}
Triglycerides (mg/dl)	70 ± 28	467 ± 91^{a}	71 ± 24	210 ± 29^{a,b}
Total Cholesterol (mg/dl)	143 ± 38	252 ± 46^{a}	128 ± 36	231 ± 33

$^{a}P < 0.05$ versus SS rats within the same treatment.
$^{b}P < 0.05$ versus vehicle-treated rats within the same strain.

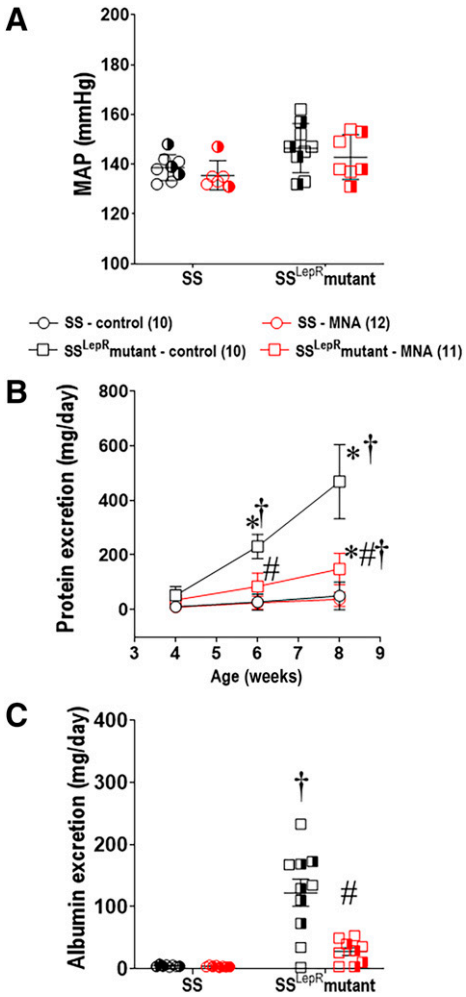

Fig. 3. Effects of chronic treatment with an MNA on MAP and markers of renal injury in SS and obese SS^{LepR}mutant rats. Control SS and SS^{LepR}mutant rats are represented by circles and squares outlined in black, respectively, and MNA-treated rats are represented by circles and squares outlined in red. Female and male rats in each group are represented by partially filled and open symbols, respectively. (A) MAP, (B) temporal changes in proteinuria, and (C) albumin excretion. Values are means ± S.D. The significance of the difference in mean values for a single timepoint was determined by a two-way ANOVA followed by Holm-Sidak's multiple comparisons test. Temporal changes in protein excretion were compared between and within groups using three-way ANOVA followed by a Tukey's multiple-comparisons test. $P < 0.05$ was considered significantly different. *, a significant difference from the corresponding value within the same strain at baseline; †, a significant difference from the corresponding value in SS rats within the same treatment; #, a significant difference from the corresponding value in control-treated rats within the same strain.

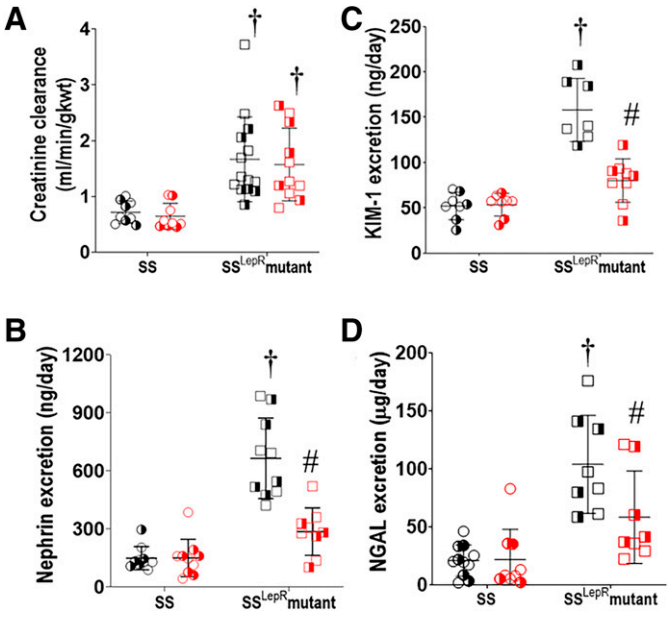

Fig. 4. Effects of chronic treatment with an MNA on creatinine clearance and markers of glomerular and tubular injury. Control SS and SS^{LepR}mutant rats are represented by circles and squares outlined in black, respectively, and MNA-treated rats are represented by circles and squares outlined in red. Female and male rats in each group are represented by partially filled and open symbols, respectively. (A) Creatinine clearance, (B) nephrin excretion, (C) KIM-1, and (D) NGAL. Values are means ± S.D. The significance of the difference in mean values for a single timepoint was determined by a two-way ANOVA followed by Holm-Sidak's multiple comparisons test. $P < 0.05$ was considered significantly different. †, a significant difference from the corresponding value in SS rats within the same treatment; #, a significant difference from the corresponding value in control-treated rats within the same strain.

hyperinsulinemia and insulin resistance. Hyperinsulinemia and insulin resistance may, in part, contribute to dyslipidemia seen in SS^{LepR}mutant rats, and the reduction of plasma triglycerides in MNA-treated SS^{LepR}mutant rats may, in part, be due to decreased hyperinsulinemia and insulin resistance. These findings may be associated with the anti-inflammatory effects of MNA. Although various studies have demonstrated that improvements in insulin sensitivity are associated with weight loss (Ikeda et al., 1996; Clamp et al., 2017), chronic MNA administration did not lead to weight loss in SS^{LepR}mutant rats despite improvements in insulin sensitivity. The lack of effect of MNA on body weight in SS^{LepR}mutant rats may be due to the mutation in their leptin receptor that makes SS^{LepR} mutant rats hyperphagic, leading to increased food intake and weight gain despite the effects of MNA on insulin resistance. These data suggest that MIP3α plays a role in insulin resistance and dyslipidemia during childhood obesity.

Despite overwhelming evidence to support the role of inflammation in the development of hypertension (Olsen, 1972; Kirabo et al., 2014; Mattson, 2019; Van Beusecum et al., 2019; Fehrenbach and Mattson, 2020), we did not observe a decrease in arterial pressure when inhibiting MIP3α in SS and SS^{LepR} mutant rats. Furthermore, the inhibition of other chemokines has been shown to reduce arterial pressure by decreasing immune cell recruitment in various animal models of hypertension (Ruiz-Ortega et al., 2002; Chung and Lan, 2011; Alsheikh et al., 2020). There are three potential reasons that could explain our observation. 1) The first possible reason is the choice of diet used during the experiment. Mattson and colleagues have fed their SS rats a high-salt diet containing 4% NaCl or greater, which causes a rapid increase in arterial pressure within 3 weeks (Rudemiller et al., 2014). In the current study, both SS and SS^{LepR}mutant strains are fed a diet containing 1% NaCl, which minimized the development of hypertension in the SS strain. 2) Another potential reason is the age of the rats used in our study. Previous studies have used SS rats older than 9 weeks of age (Mattson et al., 2006). Since the current study focused on progressive renal injury prior to puberty, it is reasonable not to expect differences in arterial

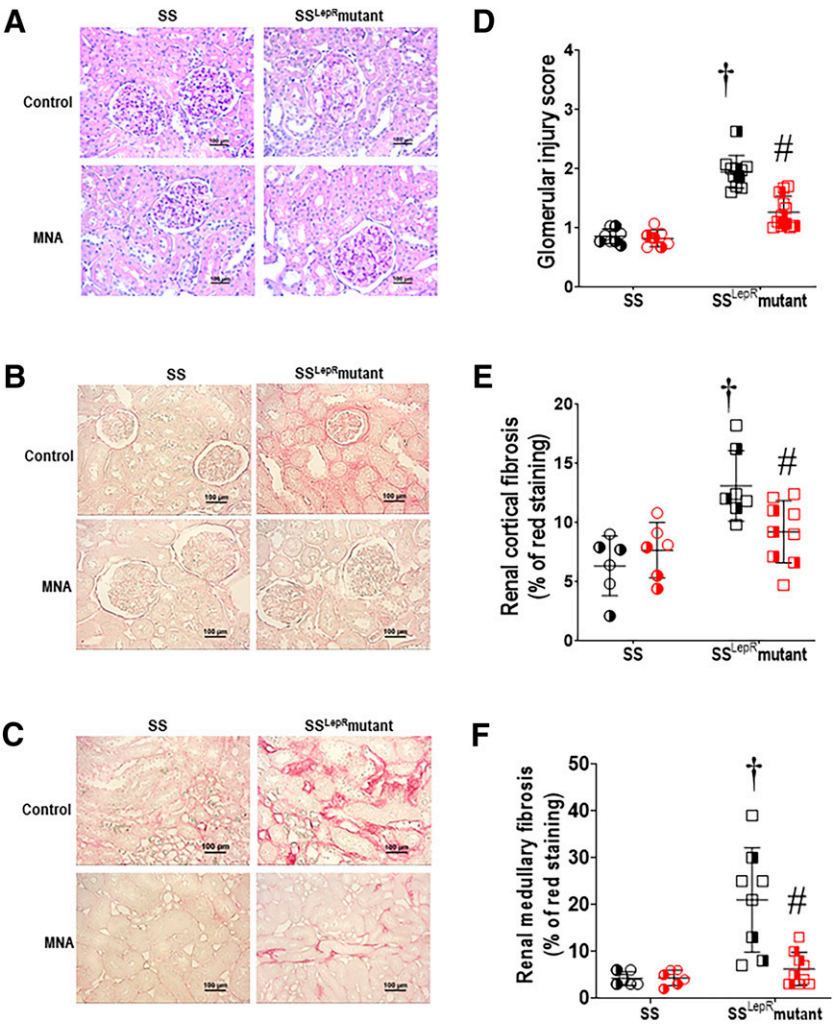

Fig. 5. Representative images and analyses of renal histopathology in SS and obese SS^{LepR}mutant rats treated with either control or an MNA. Control SS and SS^{LepR}mutant rats are represented by circles and squares outlined in black, respectively, and MNA-treated rats are represented by circles and squares outlined in red. Female and male rats in each group are represented by partially filled and open symbols, respectively. (A) Periodic acid-Schiff staining, (B) Picrosirius red staining for renal cortical fibrosis, (C) Picrosirius red staining for renal medullary fibrosis, (D) glomerular injury score, (E) renal cortical fibrosis (% of red staining), and (F) renal medullary fibrosis (% of red staining). Values are means ± S.D. The significance of the difference in mean values for a single timepoint was determined by a two-way ANOVA followed by Holm-Sidak's multiple comparisons test. $P < 0.05$ was considered significantly different. †, a significant difference from the corresponding value in SS rats within the same treatment; #, a significant difference from the corresponding value in control-treated rats within the same strain. The scale bar represents 100 μm.

pressure in response to various drugs that may typically lower arterial pressure in older animals. This is supported by recent studies from our laboratory that demonstrate that anti-inflammatory or arterial pressure–lowering drugs do not reduce arterial pressure in these rats during the prepubescent stage (Poudel et al., 2020; Brown et al., 2021). 3) The third reason is that the development of hypertension within SS rat genetic background is multifactorial, and specifically inhibiting MIP3α is not enough to reduce arterial in SS^{LepR}mutant rats. These results suggest that the lack of arterial pressure reduction in SS^{LepR}mutant rats' response to MNA administration may due to the amount of NaCl content in the diet, age, and the genetic background of the SS rats.

A significant finding from this study was that the chronic administration of MNA markedly reduced early progressive renal injury in SS^{LepR}mutant rats before puberty. Clinical and experimental studies have shown that the progressive renal injury in certain severe forms of renal disease is associated with increased renal MIP3α expression (Turner et al., 2010; Lu et al., 2017; González-Guerrero et al., 2018). MIP3α is a strong chemotactic for immune cells such as DCs, T cells, and B cells (Woltman et al., 2005; Wiede et al., 2013; Nandi et al., 2014). During renal injury, stimulatory DCs activate T cells via CD80/86 upregulation (Banchereau and Steinman, 1998; Kurts et al., 2020; Zhang et al., 2020), which elicits a proinflammatory response and macrophage recruitment, leading to renal inflammation and progressive renal injury (Kurts et al., 2020; Zhang et al., 2020). This is supported by the results of this study and preliminary reports from our laboratory demonstrating that inhibition of T-cell activation slows progressive renal injury in SS^{LepR}mutant rats before puberty (Ekperikpe et al., 2021). Therefore, we believe that chronic MIP3α neutralization with MNA reduces progressive renal injury in SS^{LepR}mutant rats by decreasing the recruitment of DCs and macrophages, thereby preventing T-cell activation. Furthermore, chronic MNA administration produces an overall anti-inflammatory effect by

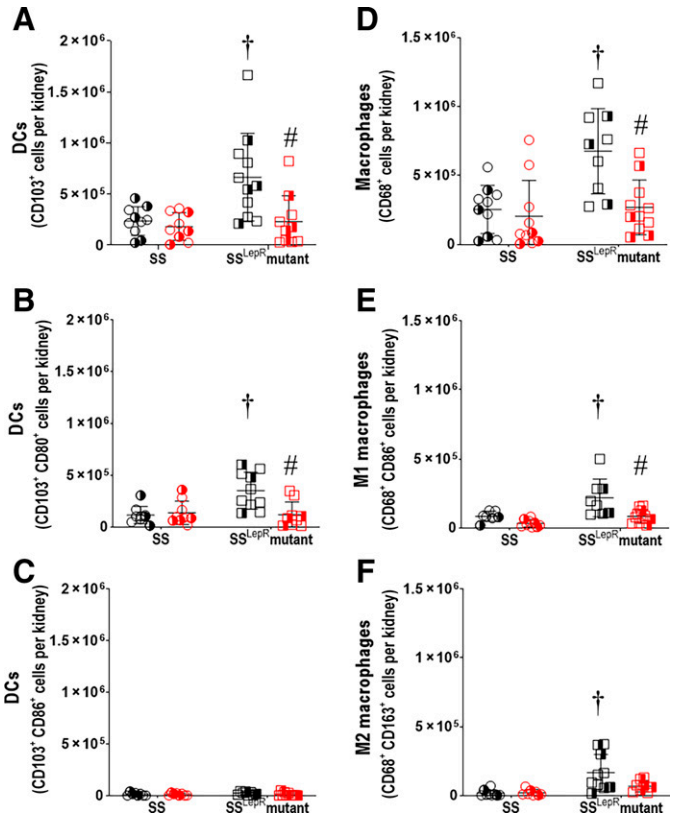

Fig. 6. Comparison of renal dendritic cell and macrophage infiltration in SS and obese SS^{LepR}mutant rats treated with either control or an MNA. Control SS and SS^{LepR}mutant rats are represented by circles and squares outlined in black, respectively, and MNA-treated rats are represented by circles and squares outlined in red. Female and male rats in each group are represented by partially filled and open symbols, respectively. (A) Dendritic cells, (B) stimulatory $CD80^+$ dendritic cells, (C) stimulatory $CD86^+$ dendritic cells, (D) total macrophages, (E) M1 macrophages, and (F) M2 macrophages. Values are means ± S.D. The significance of the difference in mean values for a single timepoint was determined by a two-way ANOVA followed by Holm-Sidak's multiple comparisons test. $P < 0.05$ was considered significantly different. †, a significant difference from the corresponding value in SS rats within the same treatment; #, a significant difference from the corresponding value in control-treated rats within the same strain.

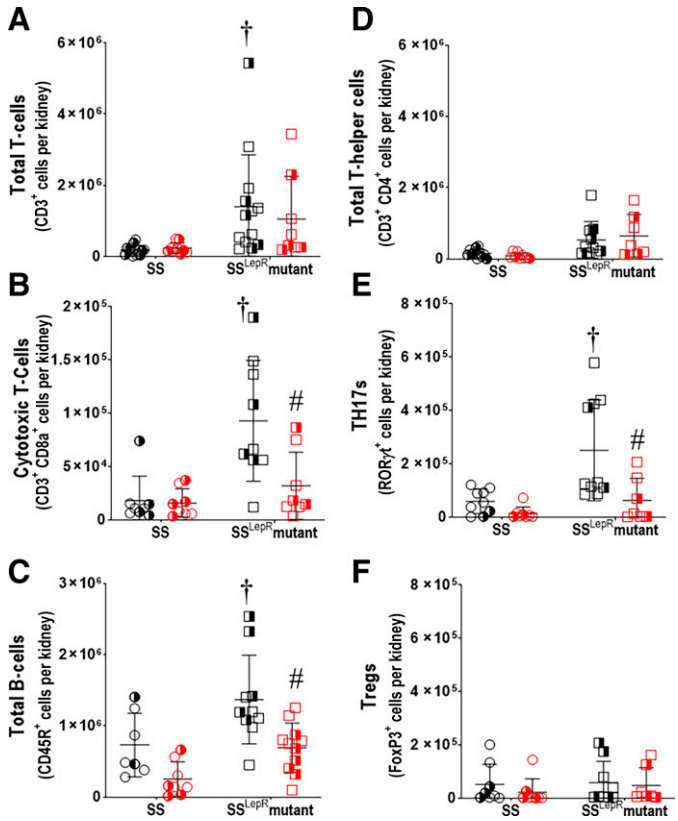

Fig. 7. Comparison of renal lymphocyte infiltration in SS and obese SS^{LepR}mutant rats treated with either control or an MNA. Control SS and SS^{LepR}mutant rats are represented by circles and squares outlined in black, respectively, and MNA-treated rats are represented by circles and squares outlined in red. Female and male rats in each group are represented by partially filled and open symbols, respectively. (A) Total T cells, (B) cytotoxic T cells, (C) B cells, (D) T helper cells, (E) IL-17–producing T cells (Th17s), and (F) regulatory T cells (Tregs). Values are means ± S.D. The significance of the difference in mean values for a single timepoint was determined by a two-way ANOVA followed by Holm-Sidak's multiple comparisons test. $P < 0.05$ was considered significantly different. †, a significant difference from the corresponding value in SS rats within the same treatment; #, a significant difference from the corresponding value in control-treated rats within the same strain.

reducing renal MIP3α expression. Although treatment with MNA decreased renal Th17 infiltration, there were no noticeable differences in renal IL-17 expression. A plausible explanation for this observation is that there are multiple sources of IL-17 other than Th17s (Keijsers et al., 2014). Overall, these data reveal that MIP3α contributes to progressive renal injury in SS^{LepR}mutant rats by mediating proinflammatory response during prepubertal obesity.

In conclusion, the data from this study suggest that during the early stages of renal injury in SS^{LepR}mutant rats, renal hyperfiltration damages glomerular and tubular epithelial cells. These cells secrete MIP3α, leading to the recruitment of DCs, which activate T cells, causing a proinflammatory response and macrophage recruitment, stimulating renal inflammation and progressive renal injury associated with obesity prior to puberty. Moreover, chronic MIP3α inhibition ameliorated metabolic syndrome and renal injury in obese SS^{LepR}mutant rats by decreasing renal inflammation. Although the current study specifically focused on the effects of MIP3α blockade on renal injury in young obese SS^{LepR}mutant rats, we would speculate that similar results would be observed in older SS^{LepR}mutant rats. Inflammation is known to contribute to renal injury in various adult animal models of obesity (Fernández-Sánchez et al., 2011; Wang et al., 2015; Lindfors et al., 2021). To the best of our knowledge, this is the first study to demonstrate a role for MIP3α in the early development of renal injury associated with obesity. Future studies from our laboratory will focus on downstream events after MIP3α-signaling stimulation during the early progression of obesity-induced renal injury such as T cell activation. These data indicate that MIP3α may be a pharmacological target for managing renal injury and metabolic disease associated with childhood obesity.

The content is solely the responsibility of the authors and does not necessarily represent the official views of the National Institutes of Health.

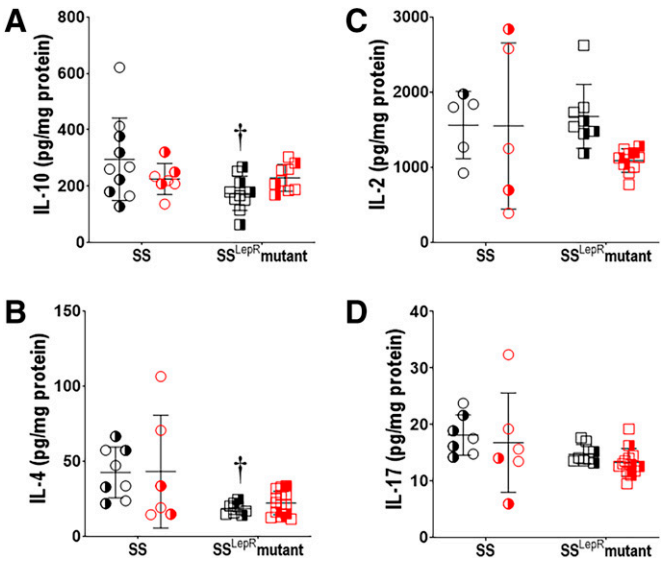

Fig. 8. Effects of chronic treatment with an MNA on the expression of renal cytokines in SS and SS^{LepR}mutant rats. Control SS and SS^{LepR} mutant rats are represented by circles and squares outlined in black, respectively, and MNA-treated rats are represented by circles and squares outlined in red. Female and male rats in each group are represented by partially filled and open symbols, respectively. (A) IL-10, (B) IL-4, (C) IL-2, and (D) IL-17. Values are means ± S.D. The significance of the difference in mean values for a single timepoint was determined by a two-way ANOVA followed by Holm-Sidak's multiple comparisons test. $P < 0.05$ was considered significantly different. †, a significant difference from the corresponding value in SS rats within the same treatment; #, a significant difference from the corresponding value in control-treated rats within the same strain.

Acknowledgments

The authors are grateful to Tyler D. Johnson and Sarah M. Safir for maintaining the animal colony.

Authorship Contributions

Participated in research design: Ekperikpe, Cornelius, Williams.

Conducted experiments: Ekperikpe, Poudel, Shields, Cornelius, Williams.

Performed data analysis: Ekperikpe, Cornelius, Williams.

Wrote or contributed to the writing of the manuscript: Ekperikpe, Mandal, Cornelius, Williams.

References

Alsheikh AJ, Dasinger JH, Abais-Battad JM, Fehrenbach DJ, Yang C, Cowley Jr AW, and Mattson DL (2020) CCL2 mediates early renal leukocyte infiltration during salt-sensitive hypertension. *Am J Physiol Renal Physiol* **318**:F982–F993.

Banchereau J and Steinman RM (1998) Dendritic cells and the control of immunity. *Nature* **392**:245–252.

Brown AK, Nichols A, Coley CA, Ekperikpe US, McPherson KC, Shields CA, Poudel B, Cornelius DC, and Williams JM (2021) Treatment With Lisinopril Prevents the Early Progression of Glomerular Injury in Obese Dahl Salt-Sensitive Rats Independent of Lowering Arterial Pressure. *Front Physiol* **12**:765305.

Burke SJ, Karlstad MD, Regal KM, Sparer TE, Lu D, Elks CM, Grant RW, Stephens JM, Burk DH, and Collier JJ (2015) CCL20 is elevated during obesity and differentially regulated by NF-κB subunits in pancreatic β-cells. *Biochim Biophys Acta* **1849**:637–652.

Cancello R, Henegar C, Viguerie N, Taleb S, Poitou C, Rouault C, Coupaye M, Pelloux V, Hugol D, Bouillot JL, et al. (2005) Reduction of macrophage infiltration and chemoattractant gene expression changes in white adipose tissue of morbidly obese subjects after surgery-induced weight loss. *Diabetes* **54**:2277–2286.

Cattaneo A, Monasta L, Stamatakis E, Lioret S, Castetbon K, Frenken F, Manios Y, Moschonis G, Savva S, Zaborskis A, et al. (2010) Overweight and obesity in infants and pre-school children in the European Union: a review of existing data. *Obes Rev* **11**:389–398.

Chung AC and Lan HY (2011) Chemokines in renal injury. *J Am Soc Nephrol* **22**:802–809.

Clamp LD, Hume DJ, Lambert EV, and Kroff J (2017) Enhanced insulin sensitivity in successful, long-term weight loss maintainers compared with matched controls with no weight loss history. *Nutr Diabetes* **7**:e282.

Czech MP (2017) Insulin action and resistance in obesity and type 2 diabetes. *Nat Med* **23**:804–814.

Czech MP, Tencerova M, Pedersen DJ, and Aouadi M (2013) Insulin signalling mechanisms for triacylglycerol storage. *Diabetologia* **56**:949–964.

Eirin A, Saad A, Woollard JR, Juncos LA, Calhoun DA, Tang H, Lerman A, Textor SC, and Lerman LO (2017) Glomerular Hyperfiltration in Obese African American Hypertensive Patients Is Associated With Elevated Urinary Mitochondrial-DNA Copy Number. *Am J Hypertens* **30**:1112–1119.

Ekperikpe US, Shields C, Brown AK, Poudel B, Cornelius DC, and Williams JM (2021) Abstract 42: Inhibiting Stimulatory Dendritic Cells Reduces Early Progressive Proteinuria In Obese Dahl Salt-sensitive Rats. *Hypertension* **78** (Suppl_1):A42.

Fehrenbach DJ and Mattson DL (2020) Inflammatory macrophages in the kidney contribute to salt-sensitive hypertension. *Am J Physiol Renal Physiol* **318**:F544–F548.

Fernández-Sánchez A, Madrigal-Santillán E, Bautista M, Esquivel-Soto J, Morales-González A, Esquivel-Chirino C, Durante-Montiel I, Sánchez-Rivera G, Valadez-Vega C, and Morales-González JA (2011) Inflammation, oxidative stress, and obesity. *Int J Mol Sci* **12**:3117–3132.

Ferris M, Hogan SL, Chin H, Shoham DA, Gipson DS, Gibson K, Yilmaz S, Falk RJ, and Jennette JC (2007) Obesity, albuminuria, and urinalysis findings in US young adults from the Add Health Wave III study. *Clin J Am Soc Nephrol* **2**:1207–1214.

González-Guerrero C, Morgado-Pascual JL, Cannata-Ortiz P, Ramos-Barron MA, Gómez-Alamillo C, Arias M, Mezzano S, Egido J, Ruiz-Ortega M, Ortiz A, et al. (2018) CCL20 blockade increases the severity of nephrotoxic folic acid-induced acute kidney injury. *J Pathol* **246**:191–204.

Hostetter TH, Rennke HG, and Brenner BM (1982) The case for intrarenal hypertension in the initiation and progression of diabetic and other glomerulopathies. *Am J Med* **72**:375–380.

Hu J, Yang Z, Li X, and Lu H (2016) C-C motif chemokine ligand 20 regulates neuroinflammation following spinal cord injury via Th17 cell recruitment. *J Neuroinflammation* **13**:162.

Huber J, Kiefer FW, Zeyda M, Ludvik B, Silberhumer GR, Prager G, Zlabinger GJ, and Stulnig TM (2008) CC chemokine and CC chemokine receptor profiles in visceral and subcutaneous adipose tissue are altered in human obesity. *J Clin Endocrinol Metab* **93**:3215–3221.

Ikeda T, Gomi T, Hirawa N, Sakurai J, and Yoshikawa N (1996) Improvement of insulin sensitivity contributes to blood pressure reduction after weight loss in hypertensive subjects with obesity. *Hypertension* **27**:1180–1186.

Kamei N, Tobe K, Suzuki R, Ohsugi M, Watanabe T, Kubota N, Ohtsuka-Kowatari N, Kumagai K, Sakamoto K, Kobayashi M, et al. (2006) Overexpression of monocyte chemoattractant protein-1 in adipose tissues causes macrophage recruitment and insulin resistance. *J Biol Chem* **281**:26602–26614.

Kanda H, Tateya S, Tamori Y, Kotani K, Hiasa K, Kitazawa R, Kitazawa S, Miyachi H, Maeda S, Egashira K, et al. (2006) MCP-1 contributes to macrophage infiltration into adipose tissue, insulin resistance, and hepatic steatosis in obesity. *J Clin Invest* **116**:1494–1505.

Kaneko K, Kimata T, Tsuji S, Shiraishi K, Yamauchi K, Murakami M, and Kitagawa T (2011) Impact of obesity on childhood kidney. *Pediatr Rep* **3**:e27.

Kasiske BL and Napier J (1985) Glomerular sclerosis in patients with massive obesity. *Am J Nephrol* **5**:45–50.

Keijsers RRMC, Joosten I, van Erp PEJ, Koenen HJPM, and van de Kerkhof PCM (2014) Cellular sources of IL-17 in psoriasis: a paradigm shift? *Exp Dermatol* **23**:799–803.

Kirabo A, Fontana V, de Faria AP, Loperena R, Galindo CL, Wu J, Bikineyeva AT, Dikalov S, Xiao L, Chen W, et al. (2014) DC isoketal-modified proteins activate T cells and promote hypertension. *J Clin Invest* **124**:4642–4656.

Kitade H, Sawamoto K, Nagashimada M, Inoue H, Yamamoto Y, Sai Y, Takamura T, Yamamoto H, Miyamoto K, Ginsberg HN, et al. (2012) CCR5 plays a critical role in obesity-induced adipose tissue inflammation and insulin resistance by regulating both macrophage recruitment and M1/M2 status. *Diabetes* **61**:1680–1690.

Kovesdy CP, Furth S, and Zoccali C; World Kidney Day Steering Committee (2017) Obesity and kidney disease: Hidden consequences of the epidemic. *Indian J Nephrol* **27**:85–92.

Kramer HJ, Saranathan A, Luke A, Durazo-Arvizu RA, Guichan C, Hou S, and Cooper R (2006) Increasing body mass index and obesity in the incident ESRD population. *J Am Soc Nephrol* **17**:1453–1459.

Kurts C, Ginhoux F, and Panzer U (2020) Kidney dendritic cells: fundamental biology and functional roles in health and disease. *Nat Rev Nephrol* **16**:391–407.

Lindfors S, Polianskyte-Prause Z, Bouslama R, Lehtonen E, Mannerla M, Nisen H, Tienari J, Salmenkari H, Forsgård R, Mirtti T, et al. (2021) Adiponectin receptor agonist AdipoRon ameliorates renal inflammation in diet-induced obese mice and endotoxin-treated human glomeruli ex vivo. *Diabetologia* **64**:1866–1879.

Lu G, Zhang X, Shen L, Qiao Q, Li Y, Sun J, and Zhang J (2017) CCL20 secreted from IgA1-stimulated human mesangial cells recruits inflammatory Th17 cells in IgA nephropathy. *PLoS One* **12**:e0178352.

Mattson DL (2019) Immune mechanisms of salt-sensitive hypertension and renal end-organ damage. *Nat Rev Nephrol* **15**:290–300.

Mattson DL, James L, Berdan EA, and Meister CJ (2006) Immune suppression attenuates hypertension and renal disease in the Dahl salt-sensitive rat. *Hypertension* **48**:149–156.

McPherson KC, Shields CA, Poudel B, Fizer B, Pennington A, Szabo-Johnson A, Thompson WL, Cornelius DC, and Williams JM (2019) Impact of obesity as an independent risk factor for the development of renal injury: implications from rat models of obesity. *Am J Physiol Renal Physiol* **316**:F316–F327.

McPherson KC, Shields CA, Poudel B, Johnson AC, Taylor L, Stubbs C, Nichols A, Cornelius DC, Garrett MR, and Williams JM (2020) Altered renal hemodynamics is associated with glomerular lipid accumulation in obese Dahl salt-sensitive leptin receptor mutant rats. *Am J Physiol Renal Physiol* **318**:F911–F921.

McPherson KC, Taylor L, Johnson AC, Didion SP, Geurts AM, Garrett MR, and Williams JM (2016) Early development of podocyte injury independently of hyperglycemia and elevations in arterial pressure in nondiabetic obese Dahl SS leptin receptor mutant rats. *Am J Physiol Renal Physiol* **311**:F793–F804.
Nandi B, Pai C, Huang Q, Prabhala RH, Munshi NC, and Gold JS (2014) CCR6, the sole receptor for the chemokine CCL20, promotes spontaneous intestinal tumorigenesis. *PLoS One* **9**:e97566.
Neels JG, Badeanlou L, Hester KD, and Samad F (2009) Keratinocyte-derived chemokine in obesity: expression, regulation, and role in adipose macrophage infiltration and glucose homeostasis. *J Biol Chem* **284**:20692–20698.
Ogden CL, Carroll MD, Fryar CD, and Flegal KM (2015) Prevalence of Obesity Among Adults and Youth: United States, 2011-2014. *NCHS Data Brief* (219):1–8.
Ogden CL, Carroll MD, Lawman HG, Fryar CD, Kruszon-Moran D, Kit BK, and Flegal KM (2016) Trends in Obesity Prevalence Among Children and Adolescents in the United States, 1988-1994 Through 2013-2014. *JAMA* **315**:2292–2299.
Olsen F (1972) Inflammatory cellular reaction in hypertensive vascular disease in man. *Acta Pathol Microbiol Scand [A]* **80**:253–256.
Önerli Salman D, Şöklar Z, Çullas İlarslan EN, Özçakar ZB, Kocaay P, and Berberoğlu M (2019) Evaluation of Renal Function in Obese Children and Adolescents Using Serum Cystatin C Levels, Estimated Glomerular Filtration Rate Formulae and Proteinuria: Which is most Useful? *J Clin Res Pediatr Endocrinol* **11**:46–54.
Ota T (2013) Chemokine systems link obesity to insulin resistance. *Diabetes Metab J* **37**:165–172.
Petersen MC and Shulman GI (2018) Mechanisms of Insulin Action and Insulin Resistance. *Physiol Rev* **98**:2133–2223.
Poudel B, Shields CA, Brown AK, Ekperikpe U, Johnson T, Cornelius DC, and Williams JM (2020) Depletion of macrophages slows the early progression of renal injury in obese Dahl salt-sensitive leptin receptor mutant rats. *Am J Physiol Renal Physiol* **318**:F1489–F1499.
Poudel B, Shields CA, Ekperikpe US, Brown AK, Travis OK, Maury JC, Fitzgerald S, Smith SV, Cornelius DC, and Williams JM (2022) The SS^{LepR} mutant rat represents a novel model to study obesity-induced renal injury before puberty. *Am J Physiol Regul Integr Comp Physiol* **322**:R299–R308.
Rayego-Mateos S, Morgado-Pascual JL, Opazo-Ríos L, Guerrero-Hue M, García-Caballero C, Vázquez-Carballo C, Mas S, Sanz AB, Herencia C, Mezzano S, et al. (2020) Pathogenic Pathways and Therapeutic Approaches Targeting Inflammation in Diabetic Nephropathy. *Int J Mol Sci* **21**:3798.
Rudemiller N, Lund H, Jacob HJ, Geurts AM, and Mattson DL; PhysGen Knockout Program (2014) CD247 modulates blood pressure by altering T-lymphocyte infiltration in the kidney. *Hypertension* **63**:559–564.
Ruiz-Ortega M, Ruperez M, Lorenzo O, Esteban V, Blanco J, Mezzano S, and Egido J (2002) Angiotensin II regulates the synthesis of proinflammatory cytokines and chemokines in the kidney. *Kidney Int Suppl* (82):S12–S22.
Savino A, Pelliccia P, Chiarelli F, and Mohn A (2010) Obesity-related renal injury in childhood. *Horm Res Paediatr* **73**:303–311.
Spires D, Poudel B, Shields CA, Pennington A, Fizer B, Taylor L, McPherson KC, Cornelius DC, and Williams JM (2018) Prevention of the progression of renal injury in diabetic rodent models with preexisting renal disease with chronic endothelin A receptor blockade. *Am J Physiol Renal Physiol* **315**:F977–F985.
Srivastava T (2006) Nondiabetic consequences of obesity on kidney. *Pediatr Nephrol* **21**:463–470.
Turner JE, Paust HJ, Steinmetz OM, Peters A, Riedel JH, Erhardt A, Wegscheid C, Velden J, Fehr S, Mittrücker HW, et al. (2010) CCR6 recruits regulatory T cells and Th17 cells to the kidney in glomerulonephritis. *J Am Soc Nephrol* **21**:974–985.
Van Beusecum JP, Barbaro NR, McDowell Z, Aden LA, Xiao L, Pandey AK, Itani HA, Himmel LE, Harrison DG, and Kirabo A (2019) High Salt Activates $CD11c^+$ Antigen-Presenting Cells via SGK (Serum Glucocorticoid Kinase) 1 to Promote Renal Inflammation and Salt-Sensitive Hypertension. *Hypertension* **74**:555–563.
van Bommel EJM, Ruiter D, Muskiet MHA, van Baar MJB, Kramer MHH, Nieuwdorp M, Joles JA, Bjornstad P, and van Raalte DH (2020) Insulin Sensitivity and Renal Hemodynamic Function in Metformin-Treated Adults With Type 2 Diabetes and Preserved Renal Function. *Diabetes Care* **43**:228–234.
Wang C, Blough E, Arvapalli R, Dai X, Triest WE, Leidy JW, Masannat Y, and Wu M (2015) Acetaminophen attenuates glomerulosclerosis in obese Zucker rats via reactive oxygen species/p38MAPK signaling pathways. *Free Radic Biol Med* **81**:47–57.
Weisberg SP, Hunter D, Huber R, Lemieux J, Slaymaker S, Vaddi K, Charo I, Leibel RL, and Ferrante Jr AW (2006) CCR2 modulates inflammatory and metabolic effects of high-fat feeding. *J Clin Invest* **116**:115–124.
Wiede F, Fromm PD, Comerford I, Kara E, Bannan J, Schuh W, Ranasinghe C, Tarlinton D, Winkler T, McColl SR, et al. (2013) CCR6 is transiently upregulated on B cells after activation and modulates the germinal center reaction in the mouse. *Immunol Cell Biol* **91**:335–339.
Woltman AM, de Fijter JW, van der Kooij SW, Jie KE, Massacrier C, Caux C, Daha MR, and van Kooten C (2005) MIP-3alpha/CCL20 in renal transplantation and its possible involvement as dendritic cell chemoattractant in allograft rejection. *Am J Transplant* **5**:2114–2125.
Zhang F, Wang C, Wen X, Chen Y, Mao R, Cui D, Li L, Liu J, Chen Y, Cheng J, et al. (2020) Mesenchymal stem cells alleviate rat diabetic nephropathy by suppressing $CD103^+$ DCs-mediated $CD8^+$ T cell responses. *J Cell Mol Med* **24**:5817–5831.

Address correspondence to: Dr. Jan M. Williams, Department of Pharmacology and Toxicology, University of Mississippi Medical Center, 2500 North State Street, Jackson, MS 39216. E-mail: jmwilliams5@umc.edu